Hyperconjugation: The Electronic Mechanism That May Underlie the Karplus Curve of Vicinal NMR Indirect Spin Couplings

Patricio F. Provasi, Carlos A. Gómez, and Gustavo A. Aucar*

Department of Physics, Northeastern University, Av. Libertad 5500, (3400) Corrientes, Argentina

Received: October 6, 2003; In Final Form: April 30, 2004

The electronic origin of the Karplus-type behavior of vicinal NMR *J* couplings for $H_3X-C_2H_4-XH_3$, X = C, Sn model compound is analyzed within the framework of the polarization propagator formalism. It is shown that its whole pattern can be understood by generalizing previous hyperconjugative mechanisms, in such a way that the hyperconjugative delocalization effect from an excitation $\sigma \rightarrow \sigma^*$ should be replaced by two simultaneous excitations according to a second-order electronic property. All and the main *coupling pathway* which involve, at the random phase level of approach, RPA, the two pairs of localized MOs closest to the coupled nuclei follows a Karplus-type dependence with dihedral X−C−C−X angle, θ. The specific two-electron integrals which include correlation at RPA level of approach are the main factors which define the total behavior of *J*. The Karplus-type dependence is also found at HF level for individual *coupling pathways* though that is not observed for the total *J*; the so-called nonlocal "perturbators" together with the inverse of the differences of energies define, at this level of approach, the functional dependence with θ.

1. Introduction

From the pioneering work of Karplus[1,2] which dealt with the dihedral angle dependence of vicinal *J* coupling (i.e., NMR indirect coupling through three bonds) between two nuclear spins of protons and then was extended to several other nuclear spins which follow the same relationships (values taken from experiments and calculations),[3,4] the use of vicinal *J* couplings for the structural elucidation and conformational analysis of molecules in solution has received increased attention.[3] That dependence is known as "Karplus' rule"; it depends parametrically on electronegativity and the relative orientation of the substituent conforming the fragment, the length of the intermediate bonds and the angles between them, molecular vibrations and electronic excitations, etc.[3] The general relationship between scalar *J* couplings and intramolecular purely quantum mechanical electronic mechanisms enforces the utility of this parameter as a sensitive local detector of quite small variations of electronic densities over the whole molecule. As an example, it was found recently that discrepancies between calculated and measured vicinal couplings can be used to reconstruct torsion angle fluctuations along the backbone of proteins.[5]

At the same time there is a growing awareness about the importance of hyperconjugation on intramolecular electronic processes, like the potential energy barriers in ethane conformation.[6] This mechanism was also used to explain in part the Karplus-type dependence of vicinal *J* couplings in ethane within the framework of finite perturbation theory.[7,8]

In this study, we use the polarization propagator formalism at the random phase level of approximation, RPA, on top of previously used semiempirical schemes.[9−11] We applied it on molecules containing heavy and nonheavy atoms. Our scheme has been able to reproduce successfully the Karplus curve for the same compounds mentioned in the title.[12] The basic scheme

was dubbed CLOPPA (contribution from localized molecular orbitals within the polarization propagator approach) by Contreras and co-workers,[13] and this is one of the most powerful schemes for the analysis of *J* couplings by *coupling pathways*. It has a natural decomposition in two different kind of operators, both having a clear physical content: the property gradient or "perturbator" [14] and the principal propagator.[15] The property gradient matrix elements corresponding to the Fermi contact, FC, mechanism are related to the density of the overlap between one occupied and one virtual MO on the nuclear site.[14] On the other side, the principal propagator matrix elements depend on the molecular electronic distribution as a whole.[15] Then the analysis of the physics underlying the transmission by the electrons through the whole molecule of the nuclear-spin−nuclear-spin interaction can be divided into two well-defined terms. In line with this, recently a new scheme for the calculation of the principal propagator as a power series[16] enhanced the capacity of analysis by the CLOPPA method. It was shown that each matrix element of the principal propagator at RPA level of approach can be expressed as a series which are functions of the inverse of a matrix containing the difference of the MO's energies and another matrix containing specific two-electron integrals. These integrals are much involved in the hyperconjugative mechanism proposed here to explain the Karplus curve.

For indirect NMR *J* couplings, the interaction between nuclear-spins mediated via electronic densities treated by the response formalism[15] requires the definition of new and more appropiate hyperconjugative mechanisms, compared with that used to explain the stabilization of ethane's staggered conformation.[6] In this case there is only one excitation $\sigma_m \rightarrow \sigma_n^*$, in the delocalization mechanism involved. What we want to address here is whether there is another way of understanding the subtle mechanism which causes the Karplus-type behavior of vicinal couplings and if that can be related with the propagation of perturbed magnetic interactions as this propagation is understood within polarization propagators. Our goal is to show that vicinal NMR *J* couplings can be rationalized as arising from purely

---

* Corresponding author. E-mail: gaa@unne.edu.ar.

hyperconjugative electronic effects though of a kind related to the second-order property analyzed.

This paper is organized as follows: In section 2, we present an overview of the polarization propagator theory and a discussion of the novel hyperconjugative mechanism we are proposing. We describe the physics that is involved by propagators within our scheme and define what a *coupling pathway* is as well as its constituents. Then we introduce the proper hyperconjugative interaction mechanism for a second-order property and some of the main hyperconjugative mechanisms of the *second kind* involved in the transmission of vicinal NMR *J* couplings. In section 3, we present an analysis of calculations considering first the behavior of the main *coupling pathways*—that is the main factors responsible for that behavior—and then the dependence of the dihedral angle of some two-electron integrals. Finally we show that within the zeroth-order approximation, ZOA, there is no Karplus type dependence for the total vicinal *J* coupling. The main conclussions are sumarized in section 4.

2. Theory

To get a deeper insight in the physics that may be obtained from the methodology we use in this work and also for the sake of completeness, we give a brief overview of polarization propagators. Propagators are two-particle double-time Green's functions. The polarization propagators are one type of propagators which can be defined as[17,18]

$$\langle\langle V(t); W(t')\rangle\rangle \equiv -i\hbar\langle 0|T\{V(t)W(t')\}|0\rangle \tag{1}$$

where T is the time-ordering operator. The object $\langle\langle;\rangle\rangle$ of eq 1 can be interpreted as the probability amplitude that a (magnetic) polarization $W(t')|0\rangle$ created at time t' will become a (magnetic) polarization $V(t)|0\rangle$ at a later time t. When $W(t')$ is a local perturbation like the interaction between a nuclear spin with electron spins there will be a local shift of the electronic spin density that will be propagated to the whole system. The effect of this perturbation in any region of the molecule can be accounted for considering another local perturbation like $V(t)$.

Within the spectral or Lehman[19] representation, the polarization propagator of eq 1 is written as

$$\langle\langle V; W\rangle\rangle_{E=0} = \sum_{n\neq0}\left[\frac{\langle 0|V|n\rangle\langle n|W|0\rangle}{E_0 - E_n} + cc\right] \tag{2}$$

This equation shows the intrinsic fundamental relationship between second-order perturbation theory and polarization propagators when matrix elements and the energy eigenvalues are exact. From the knowledge of state functions and the complete spectra of eigenvalues of the Hamiltonian corresponding to the unperturbed molecular system it is, in principle, possible to calculate $\langle\langle V; W\rangle\rangle$. However what one wants to do is to calculate eq 2 directly by some other independent procedure. From these propagators, we can get the dynamics of some perturbations acting on the electronic molecular system. Considering the equation of motion that the propagator of eq 1 must fulfill, some strategies were developed in order to obtain that propagator without solving directly eq 2. One of them is to use the superoperator formalism. Within this formalism, it is possible to solve eq 2 from an approximate reference state by truncating the projection manifold of basic excitation operators that generate the whole set of excited states. The simplest possible approximation that one can apply to get the polarization propagators up to consistent first order in the fluctuation

potential is the RPA. This is obtained when the reference state is taken as the Hartree–Fock state and the excitation manifold of operators is truncated at the particle–hole and hole–particle excitation operators.[18]

A general expression for calculating molecular properties within polarization propagator methods at RPA level of approach can be written as[15]

$$R = \Omega\tilde{\mathbf{b}}\mathbf{P}\mathbf{b} \tag{3}$$

where Ω is a constant which depends on the property studied. $\mathbf{P}$ is called the principal propagator and depends on the electronic molecular structure as a whole and also on the time reversal symmetry of the molecular property studied.[20] The matrix $\mathbf{b}$ and its transpose $\tilde{\mathbf{b}}$ are called the property matrices or "perturbators".[14] Singlet or triplet type property matrix elements are given by

$$\mathbf{b}_{ia} = \langle i|V|a\rangle \tag{4}$$

where V stands for the perturbation related with the property studied. For example, for the FC contribution to the *J* coupling, we have

$$V^{FC} = \frac{8h\beta}{3}\sum_X\gamma_X\sum_k\delta(r_{kX})(s_k\cdot\mathbf{I}_X) \tag{5}$$

where r_{kX} is the position vector from the nucleus X to the kth electron, s_k is its electron-spin operator and β is the Bohr magneton.

At the RPA level of approach the principal propagator matrix is built up from the following matrix elements

$$^m\mathbf{P}_{ia,jb} = (^m\mathbf{A} \pm {}^m\mathbf{B})_{ia,jb}^{-1} \tag{6}$$

where $m = 1$ (3) for singlet (triplet) type properties. When $m = 1$ (3) the $+$ $(-)$ sign between $^1\mathbf{A}$ ($^3\mathbf{A}$) and $^1\mathbf{B}$ ($^3\mathbf{B}$) is applied. The explicit matrix elements for $\mathbf{A}$ and $\mathbf{B}$ matrices are[15]

$$^1\mathbf{A}_{ia,jb} = (\epsilon_a - \epsilon_i)\delta_{ab}\delta_{ji} + 2\langle aj|ib\rangle - \langle aj|bi\rangle \tag{7}$$

$$^3\mathbf{A}_{ia,jb} = (\epsilon_a - \epsilon_i)\delta_{ab}\delta_{ji} - \langle aj|bi\rangle \tag{8}$$

$$^1\mathbf{B}_{ia,jb} = \langle ab|ji\rangle - 2\langle ab|ij\rangle \tag{9}$$

$$^3\mathbf{B}_{ia,jb} = \langle ab|ji\rangle \tag{10}$$

The indices i, j (a, b) account for occupied (virtual) molecular orbitals; ϵ_i (ϵ_a) represent their corresponding energies, and the other elements are two-electron integrals. If real wave functions are considered, the two-electron integrals are here expressed within the "physicist" notation as

$$\langle ia| jb\rangle = \int\psi_i(1)\psi_j(1)r_{12}^{-1}\,\psi_a(2)\psi_b(2)\,d\mathbf{r}_1\,d\mathbf{r}_2 \tag{11}$$

The indirect nuclear-spin *J* coupling is mediated via electrons. It arise from the interaction ("external" perturbation) of each nuclear-spin with its electronic environment. The information on the way a magnetic perturbation originated in one nucleus is transmitted to all other nuclear sites is stored in the matrix elements of eqs 4 and 6. The matrix elements of the principal propagator are defined by MO energies and two-electron integrals of eqs 7–10, which are obtained from the description of the unperturbed system. Then there are inside themselves, as a propensity, the stream lines by which local perturbations

Hyperconjugation

J. Phys. Chem. A, Vol. 108, No. 29, 2004 **6233**
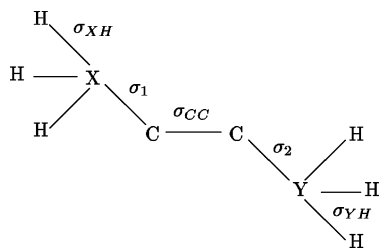
Figure 1. Scheme of compounds analyzed and some localized MOs.

are transmitted to the whole molecule. Those perturbations may or may not depend on electron's spins.

2.1. The CLOPPA-Z Scheme and *Coupling Pathways*. The CLOPPA-Z (Z = INDO, MNDO, AM1, INDO/S)[13,9,10,11] semiempirical scheme was developed to get semiquantitative reproduction of NMR-*J* couplings. All four contributions, i.e. diamagnetic spin−orbit, DSO, paramagnetic spin−orbit, PSO, spin-dipolar, SD, and Fermi contact, FC, can be calculated. The calculations start from the knowledge of the electronic description of the molecular system at a defined semiempirical "Z" level of approach. Then the polarization propagator formalism is applied including only two new parameters: $S_X^2(0)$, the electronic density of atomic *s*-type orbitals corresponding to the atom X for the FC mechanism, and the average $\langle r_X^{-3} \rangle$ for the other two paramagnetic mechanisms, PSO and SD. These parameters are taken from *ab initio* calculations on the atom X.[21] Relativistic effects are included in this way on the principal propagator (through the Z scheme of parametrization) and also on the "perturbators" (e.g. through $S_X^2(0)$), for calculations of J^{FC} within the CLOPPA-MNDO scheme.[9]

The NMR coupling constant between two nuclei X and Y calculated with the CLOPPA scheme is expressed as a sum of contributions of different *coupling pathways*, i.e., $J_{ia,jb}$ defined by four localized MOs, LMOs. The total *J* coupling is expressed as a sum of a paramagnetic and a diamagnetic part. The paramagnetic term can be written as

$$J(X, Y) = \sum_{ia, jb} J_{ia,jb} \qquad (12)$$

where three different mechanisms contribute to each $J_{ia,jb}$ term. The fourth mechanism, i.e. the diamagnetic contribution is usually obtained as a ground-state expectation value.

We studied only the FC interaction because this is by far the most important one for the vicinal coupling ^3J(X, Y; X, Y = C, Si, Sn, Pb) in $H_3X-H_2CCH_2-YH_3$ model compounds (see Figure 1).

Each coupling term $J_{ia,jb}$ can be expressed as[14]

$$J_{ia,jb}^{(X,Y)} = \Omega\{\mathbf{V}_{ia,X}\mathbf{V}_{jb,Y} + \mathbf{V}_{ia,Y}\mathbf{V}_{jb,X}\}\mathbf{P}_{ia,jb} \qquad (13)$$

where $\mathbf{P}_{ia,jb}$ is the *ia*, *jb* matrix element of the principal propagator matrix and $V_{ia,X}$ is the property matrix element of the so-called "perturbator" at the site of nucleus X.[14] Each term of eq 13 was calculated in this work by the CLOPPA-MNDO method.[9] This method was previously applied to calculate coupling constants in different model compounds.[9,12,14] Its performance was satisfactory in general for couplings involving nuclear spins of H and C, and gave semiquantitative and reliable reproduction of experimental values for ^3J(Sn, Sn) in $H_3Sn-H_2CCH_2-SnH_3$.[12]

Because of the fact that the principal propagator results from the inverse of a large matrix in ab initio calculations when both correlation and large basis sets are taken care of this matrix cannot be calculated directly; an indirect procedure was then

developed to overcome this problem,[22] but in this way, unfortunately, the physical information stored in that matrix is lost.

To keep the physical meaning for each matrix element of **P**, a new procedure was recently proposed.[16] It is such that the principal propagator can be written as

$$(^m\mathbf{P}_S)_{ia,jb} = [\mathbf{E}^{-1}(\mathbf{I} - {}^m\mathbf{N}\mathbf{E}^{-1})^{-1}]_{ia,jb} \qquad (14)$$

$$= \mathbf{E}^{-1}\sum_{i=0}^{\infty}(({}^m\mathbf{N}\mathbf{E}^{-1})^i)_{ia,jb} \qquad (15)$$

$$\approx (\mathbf{E}^{-1}\sum_{n=0}^{p}({}^m\mathbf{N}\mathbf{E}^{-1})^n)_{ia,jb} = (^m\mathbf{P}_S)_{ia,jb;p} \qquad (16)$$

where *p* stands for the number of terms considered for each series; **E** is a diagonal matrix (when canonical MOs are used) built up from the difference of MOs energies, and $^m\mathbf{N}$ means the two-electron integrals given in eqs 7−10. Each matrix element of the matrix obtained as a product between $^m\mathbf{N}$ and $\mathbf{E}^{-1}$ can be written as

$$v_{ia,jb} = ({}^m\mathbf{N}\mathbf{E}^{-1})_{ia,jb} \qquad (17)$$

and convergence of each series is ensured when

$$|v_{ia,jb}^{max}| < 1 \qquad (18)$$

being $v_{ia,jb}^{max}$ the maximum value of all $v_{ia,jb}$. The algorithm employed in our code to generate the matrix **P** is based on the partial summation

$$S_p = \sum_{i=0}^{p} v^i \qquad (19)$$

Then

$$S_p = S_{p-1} + v^{2(p-1)}S_{p-1} \qquad (20)$$

In a similar manner it is possible to generate the matrix **P** by splitting it up in two parts: one diagonal, named $\mathbf{P}_d$ and another nondiagonal, named $\mathbf{P}_{nd}$ as was done for the generation of the energy matrix $\mathbf{E}^{-1}$ in ref 16.

Each matrix element of the principal propagator written as a series has its own rate of convergence.[16] Moreover, there is another very important point that arises from eq 16: each matrix element of **P** is a power series in **N**. Then they will be function of two-electron integrals and also of the inverse of the energy matrix, **E**. This will be explained in more details in sections 3.3 and 3.4.

2.2. Previous NJC Description. Recently hyperconjugative delocalization effects were found to explain in part the Karplus-type dependence of vicinal *J* couplings with the dihedral angle of HC−CH in ethane within the framework of finite perturbation theory. Calculations were done applying (hybrid) density functional theory (DFT) and natural bond orbitals (NBO). This scheme was dubbed natural *J* coupling (NJC).[7,23] Weinhold and co-workers proposed two independent mechanisms for the transmission of vicinal *J* couplings: (i) steric exchange orthogonalization and (ii) hyperconjugation $\sigma_i \rightarrow \sigma_j^*$. Mechanism (i) arises from the fact that the local perturbation modifies each NBO (with electron spin α or β) differently; this modification is "propagated" by the Pauli restriction, i.e. all α and β should be orthogonal to each other. Mechanism (ii) is related to spin

hyperconjugative delocalization. Weinhold and coauthors have shown that within the NJC scheme ~70% of the vicinal *J* coupling in ethane is due to the steric exchange orthogonalization mechanism. To describe the part of *J* coupling transmitted by hyperconjugative mechanisms they introduced the non-Lewis contribution, which consists of two terms. The main one is related with delocalization effects of hyperconjugative type, which means, the electron density transfer from an occupied NBO σ_i to a virtual σ_j^* centered in some different region of the molecule. The other non-Lewis contributions corresponds to intrabond redistribution of electron density within the region of parent σ_i.

On the other hand, Contreras and co-workers have presented a restricted version of the NJC scheme. They have studied the contribution due to the electron transfer $\sigma_m \rightarrow \sigma_n^*$ to the vicinal couplings in ethane and some other couplings in different compounds.[8,24,25] In this scheme each *mn** contributions were obtained from the difference in calculated *J* couplings that arises when considering the full Fock matrix and the Fock matrix where the elements *mn** were deleted.

2.3. Valence Bond Bond Order Formulation. According to eq 35 of ref 26, within the valence bond, VB, bond order formulation the vicinal hydrogen−hydrogen NMR *J* coupling is written as

$$J_{HH'} = 4185(\Delta E)^{-1} p^0(h, h') + {}^3\!/_2 p^0(h, \sigma) p^0(\sigma', h') \quad (21)$$

where ΔE is the "mean excitation energy" and $p^0(t, u)$ is the fragment bond order. The "direct" contribution $p^0(h, h')$ should be the dominant one compared with the "indirect" contributions $p^0(h, \sigma)$ and $p^0(\sigma', h')$ for vicinal couplings. The "direct" contributions can be written as

$$p^0(h, h') = \frac{K(c, c')}{4K(c, h)} \quad (22)$$

when only nearest neighbor exchange are included. The atomic orbitals h and h' are of s-type centered on H and H' atoms, σ and σ' are atomic orbitals of sp type centered on carbon atoms pointing to each other, and c and c' are atomic orbitals of sp type pointing from carbon atoms to hydrogen atoms. $K(a, b)$ are two-electron VB exchange integrals associated with atomic orbitals a and b. The integral

$$K(c, c') = \int c(1)c'(2) r_{12}^{-1} c(2)c'(1) d\mathbf{r}_1 d\mathbf{r}_2 \quad (23)$$

has a Karplus-type dependence on θ. This means that within this approximation[26]

$$J_{HH'} \approx 4185(\Delta E)^{-1} p^0(h, h') = A \cos^2\theta + B \cos\theta + C \quad (24)$$

Weinhold and coauthors[7] argued that the steric mechanism within the NJC description mentioned above is related with the "direct" contribution within Penney−Dirac bond order scheme of Barfield and Karplus[26]

2.4. Hyperconjugative Interactions. Within the NBO scheme, the hyperconjugative electron transfer mechanisms are understood as the interactions that involves partial electron transfer from a nearly doubly occupied (bonding) orbital to a nearly vacant (antibonding) orbital. Considering the FC mechanism in a *J* coupling interaction one should expect a complex excitation pattern related to nuclear-spin/electron-spin interactions transmitted through the molecular electronic system.

We propose here a new scheme to express the hyperconjugative interactions involved in a vicinal *J* coupling which is
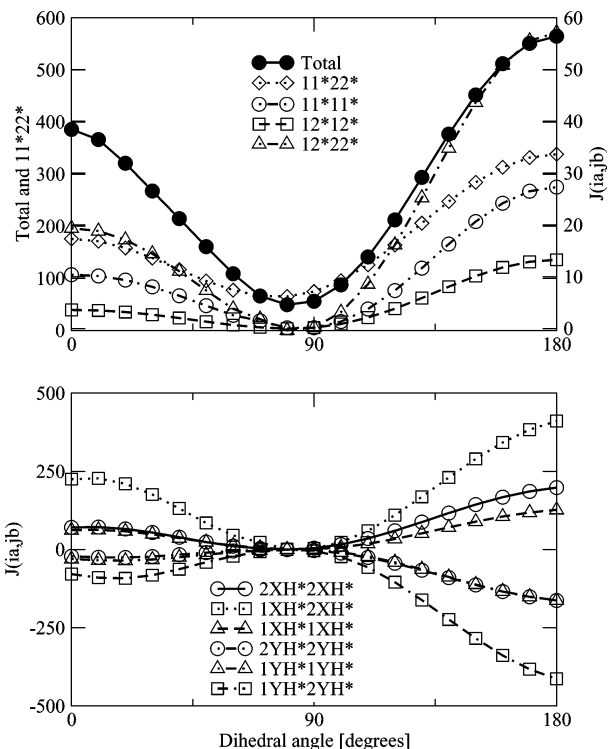

Figure 2. Contributions of some of the main couplings pathways [in Hz] for X = Y = Sn: (a) −●−, total; ···◇···, $(\sigma_1\sigma_1^*; \sigma_2\sigma_2^*)$ - -□- -, $(\sigma_1\sigma_2^*; \sigma_1\sigma_2^*)$; -·-△-·-, $(\sigma_1\sigma_2^*; \sigma_2\sigma_2^*)$; - -○ - -, $(\sigma_2\sigma_2^*; \sigma_2\sigma_2^*)$; (b) −○−, $(\sigma_2\sigma_{XH}^*; \sigma_2\sigma_{XH}^*)$; ···□···, $(\sigma_1\sigma_{XH}^*; \sigma_2\sigma_{XH}^*)$; - -△- -, $(\sigma_1\sigma_{XH}^*; \sigma_1\sigma_{XH}^*)$ - ·-○- ·-, $(\sigma_1\sigma_{YH}^*; \sigma_1\sigma_{YH}^*)$; ·· -□- ·· $(\sigma_1\sigma_{YH}^*; \sigma_2\sigma_{YH}^*)$; - - -△- - ·, $(\sigma_2\sigma_{YH}^*; \sigma_2\sigma_{YH}^*)$.

related to two simultaneous electron excitations, from occupied LMOs to vacant LMOs. We will call this mechanism hyperconjugation of the *second kind* in order to differentiate it from the one-electron excitations which we will refer to as being hyperconjugative of the *first kind*.

From the total set of *coupling pathways*, some of the main terms which contribute to the vicinal X, Y coupling as well as the total ${}^3\!J_{X-Y}^{FC}$ are shown in Figure 2. Each of them have two bonding−antibonding excitations, which means simultaneous two-electron transfer. In Figure 3, four typical electronic hyperconjugation of a *second kind* for vicinal couplings are shown. In the case of the *local local hyperconjugative* mechanism, LLH, of Figure 3a each electron transfer occurs on the same bond, being two different excitations for two different bonds. In the case of the *double vicinal hyperconjugative* mechanism, DVH, of Figure 3b both excitations start on the same bonding orbital and goes to the same antibonding orbital. The other two *coupling pathways* dubbed *double local hyperconjugative* (DLH) and *vicinal local hyperconjugative* (VLH), represented in Figure 3, parts c and d, respectively, contribute to the through bond and to a kind of mixed mechanisms.

Contributions from some other mechanisms are given in Figure 2. They involve the excitation from the bonding orbital σ_1 or σ_2 to an XH (YH) antibonding orbitals instead of the previous CX or σ_1^* (CY or σ_2^*). These six contributions are representative of the whole set of them. They are large and have, all of them, a Karplus-type behavior. They are also symmetric in such a way that they almost cancel each other.

It is worth mentioning that the contribution of each *coupling pathway* is obtained as a product of only one principal propagator matrix element and the sum of two terms containing each a product of two "perturbators"; see eq 13. So for the

Hyperconjugation

J. Phys. Chem. A, Vol. 108, No. 29, 2004 **6235**
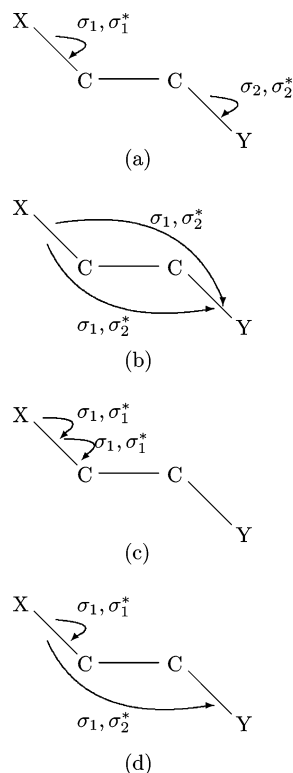
Figure 3. Some of the hyperconjugative mechanisms of the second kind that may or may not produce the Karplus-type behavior on $^3J_{(X-Y)}$: (a) local−local hyperconjugative (LLH); (b) double-vicinal hyperconjugative (DVH); (c) double-local hyperconjugative (DLH); (d) local−vicinal hyperconjugative (LVH)

contribution of the LLH *coupling pathway* there is a product of two "perturbators"

$$V_{\sigma_1\sigma_1}*,_X V_{\sigma_2\sigma_2}*,_Y \qquad (25)$$

where each of them is a local "perturbator". Its name follows because of each excitation $\sigma_i \rightarrow \sigma_i^*$ involves LMOs which resemble chemical bonds involving one of the nuclei whose coupling is under study. There is also another product of (nonlocal) "perturbators", which reads as follows

$$V_{\sigma_2\sigma_2}*,_X V_{\sigma_1\sigma_1}*,_Y \qquad (26)$$

where, as shown in Figure 1, σ_i and σ_i^* ($i = 1, 2$) are LMOs that describe the covalent C−X or C−Y bonds.

As a rule, the contribution of the local FC "perturbators" are by far the largest compared with the contribution of nonlocal "perturbators". Both "perturbators" can have quite different functional dependence with θ.

3. Results and Discussion

The geometries of the $H_3X-C_2H_4-YH_3$ model compounds were optimized using the MOPAC package of programs[27] with MNDO[28] method for X, Y = C, Sn starting in the cis conformation (0°). All other geometries were obtained by changing only the dihedral angle (XC−CY), θ.

The calculations and the analysis of all vicinal couplings were performed with the CLOPPA-MNDO scheme.[9] In Table 1 we show the contributions of some of the main *coupling pathways* to $^3J(X, Y)$, when X, Y = Sn and the dihedral angle varies in steps of 10° for the rank $0 \leq \theta \leq 180°$.

TABLE 1: Total FC Values and Some *Coupling Pathways* Contributions for $^3J_{X-Y}$ Coupling in $H_3X-C_2H_4-YH_3$ with X = Y = Sn. All Values in Hz.

angle	$^3J^{FC}_{Total}$	$^3J^{FC}_{\sigma_1\sigma_1^*\sigma_2\sigma_2^*}$	$^3J^{FC}_{\sigma_2\sigma_2^*\sigma_1\sigma_2}$	$^3J^{FC}_{\sigma_1\sigma_2^*\sigma_2\sigma_2^*}$	$^3J^{FC}_{\sigma_1\sigma_1^*\sigma_1\sigma_1^*}$
0	162.735	175.906	3.051	5.512	2.376
10	154.826	171.355	2.974	5.361	2.312
20	135.453	158.291	2.716	4.874	2.093
30	111.776	139.158	2.288	4.095	1.729
40	86.808	116.942	1.732	3.115	1.265
50	60.181	95.209	1.129	2.044	0.769
60	33.833	77.434	0.565	1.036	0.332
70	16.478	66.597	0.194	0.438	0.087
80	1.575	65.342	−0.039	−0.084	0.030
90	0.991	74.840	0.133	0.153	0.376
100	10.243	95.510	0.742	1.105	1.166
110	27.716	126.108	1.812	2.801	2.423
120	51.296	164.124	3.290	5.152	4.086
130	78.476	206.065	5.052	7.948	6.023
140	106.201	247.530	6.917	10.895	8.042
150	131.424	284.299	8.658	13.638	9.909
160	151.481	313.180	10.068	15.865	11.418
170	164.365	331.780	10.996	17.324	12.408
180	168.800	338.181	11.316	17.821	12.743

Since the general trend of the different features analyzed in this work are very similar for X = Y = C, Sn, curves are ploted only for X = Y = Sn.

3.1. Patterns of the Main Coupling Pathways. It was previously shown that the CLOPPA-MNDO scheme nicely reproduces the Karplus behavior of the vicinal Sn−Sn couplings.[12] The same happens when X, Y = C, Si and Pb. When considering the contribution of each *coupling pathway*, it is also found that all coupling terms follow the same trend. The main terms for X, Y = Sn are shown in Figure 2. They have different magnitude but the same overall behavior. One intriguing and still unsolved aspect is the reason to explain that all *coupling pathway* contributions have a minimum for $70 < \theta < 85°$, but their maximum is always at $\theta = 180°$.

3.2. Principal Propagators and Perturbators. To obtain a deeper understanding of the electronic mechanism that underlies the Karplus-type behavior of the *coupling pathways* as a function of the θ angle, we can use eq 13 together with eq 15 as powerful tools in this respect.

In Figure 4, we show the pattern of contributions belonging to the main *coupling pathway*, i.e. $\sigma_1\sigma_1^*\sigma_2\sigma_2^*$ given by each local "perturbator" and by the principal propagator matrix elements for X, Y = Sn. It is seen that the corresponding matrix elements of the principal propagator follows a Karplus-type
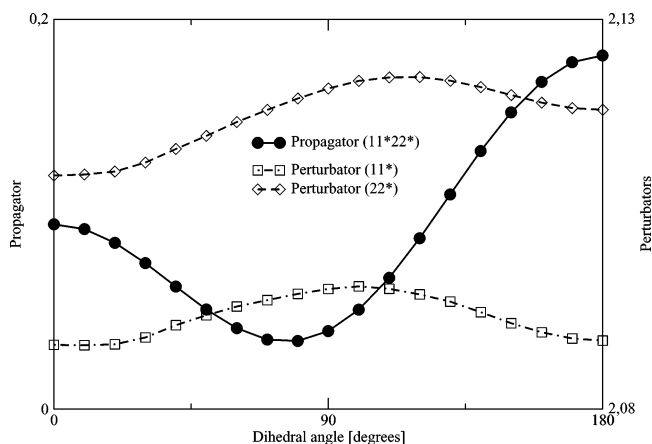
Figure 4. Principal propagator (on left axis) and two local "perturbators" (on right axis) corresponding to $\sigma_1\sigma_1^*;\sigma_2\sigma_2^*$, for X = Y = Sn: (−◇−) perturbator $\sigma_1\sigma_1^*$; (−□−) perturbator $\sigma_2\sigma_2^*$; (−●−) principal propagator.
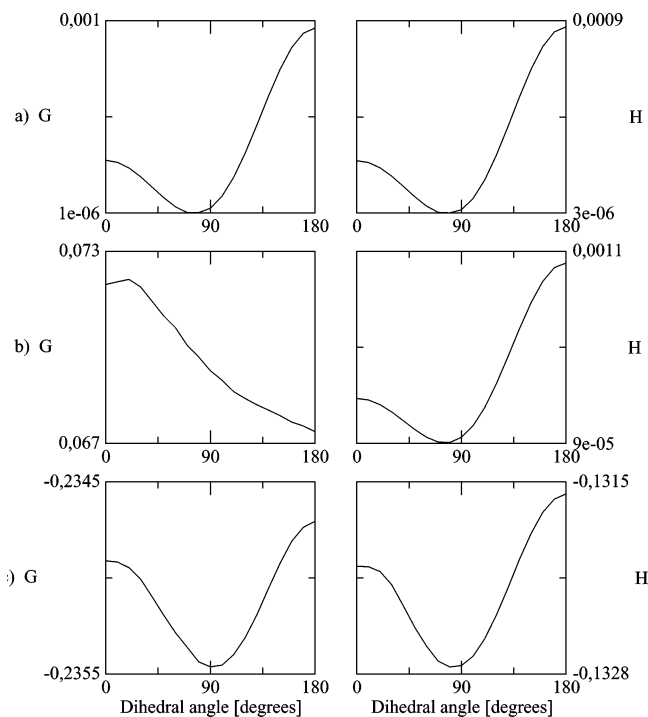
Figure 5. *G* and *H* two-electron-integrals for cases a–c for X = Y = Sn.

behavior. However, the two "perturbators" are almost constant for all dihedral angles though little larger on the right-hand side of those figures. This variation will enhance the Karplus-type behavior of the matrix element $\mathbf{P}_{\sigma_1\sigma_1*,\sigma_2\sigma_2*}$. We also found a Karplus-type curve for the product of "perturbators" calculated by eq 26. This is a product of nonlocal "perturbators" which is obtained from the overlap of $\sigma_1 \rightarrow \sigma_1^*$ on the nucleus Y and the overlap of $\sigma_2 \rightarrow \sigma_2^*$ on the nucleus X. They give a very small fraction of the total contribution of the "perturbators" term (see eqs 13 and 26).

Starting from eqs 8 and 10, we can take another step deeper into our analysis. The matrix elements of the matrix $^m\mathbf{N}$ are two-electron integrals of eqs 7–10. They are Coulombic and exchange integrals and can be explicitly written as

$$G_{\sigma_i\sigma_a*,\sigma_j\sigma_b*} = \int \sigma_a^*(1)\sigma_b^*(1)r_{12}^{-1}\sigma_j(2)\sigma_i(2)\, d\mathbf{r}_1\, d\mathbf{r}_2 \quad (27)$$

$$H_{\sigma_i\sigma_a*,\sigma_j\sigma_b*} = \int \sigma_a^*(1)\sigma_j(1)r_{12}^{-1}\sigma_b^*(2)\sigma_i(2)\, d\mathbf{r}_1\, d\mathbf{r}_2 \quad (28)$$

We have calculated both these integrals and the energy difference $\epsilon_{\sigma_1} - \epsilon_{\sigma_1*}$ as a function of dihedral angle.

Perturbators $V_{\sigma_1\sigma_1*,X}$ and $V_{\sigma_1\sigma_2*,X}$ have the explicit form

$$V_{\sigma_1\sigma_1*,X} \propto \sigma_1^*(X)\sigma_1(X) \quad (29)$$

$$V_{\sigma_1\sigma_2*,X} \propto \sigma_2^*(X)\sigma_1(X) \quad (30)$$

3.3. Pattern of Few Two-Electron Integrals and Perturbators. In Figure 3, we show four different hyperconjugative mechanism of a *second kind* that are useful in order to understand the reason for the Karplus-type behavior of the whole *J* coupling. We can try to get a deeper insight into this issue by analyzing several two-electron integrals which are involved in three typical *coupling pathways* (see Figure 5): (a) $\sigma_1\sigma_1^*\sigma_2\sigma_2^*$; (b) $\sigma_1\sigma_2^*\sigma_1\sigma_2^*$; (c) $\sigma_1\sigma_1^*\sigma_1\sigma_1^*$.

(a) In this case the integrals are written as

$$G_{\sigma_1\sigma_1*,\sigma_2\sigma_2*} = \int \sigma_1^*(1)\sigma_2^*(1)r_{12}^{-1}\sigma_2(2)\sigma_1(2)\, d\mathbf{r}_1\, d\mathbf{r}_2 \quad (31)$$

$$H_{\sigma_1\sigma_1*,\sigma_2\sigma_2*} = \int \sigma_1^*(1)\sigma_2(1)r_{12}^{-1}\sigma_2^*(2)\sigma_1(2)\, d\mathbf{r}_1\, d\mathbf{r}_2 \quad (32)$$

(b) In this case *G* and *H* are much different:

$$G_{\sigma_1\sigma_2*,\sigma_1\sigma_2*} = \int \sigma_2^*(1)\sigma_2^*(1)r_{12}^{-1}\sigma_1(2)\sigma_1(2)\, d\mathbf{r}_1\, d\mathbf{r}_2 =$$
$$\int |\sigma_2^*(1)|^2 r_{12}^{-1}|\sigma_1(2)|^2\, d\mathbf{r}_1\, d\mathbf{r}_2 \quad (33)$$

$$H_{\sigma_1\sigma_2*,\sigma_1\sigma_2*} = \int \sigma_2^*(1)\sigma_1(1)r_{12}^{-1}\sigma_2^*(2)\sigma_1(2)\, d\mathbf{r}_1\, d\mathbf{r}_2 \quad (34)$$

(c) The integrals *G* and *H* have their usual meaning

$$G_{\sigma_1\sigma_1*,\sigma_1\sigma_1*} = \int |\sigma_1^*(1)|^2 r_{12}^{-1}|\sigma_1(2)|^2\, d\mathbf{r}_1\, d\mathbf{r}_2 \quad (35)$$

$$H_{\sigma_1\sigma_1*,\sigma_1\sigma_1*} = \int \sigma_1^*(1)\sigma_1(1)r_{12}^{-1}\sigma_1^*(2)\sigma_1(2)\, d\mathbf{r}_1\, d\mathbf{r}_2 \quad (36)$$

As observed in Figure 5, in case a, both integrals have a Karplus-type behavior. This occurs also for the integral *H* in case b but not for integral G. In case c, neither of the integrals *G* or *H* has a Karplus-type behavior.

From these three typical cases it follows that the two-electron integrals (*G* and *H*) have a Karplus-type behavior only when electron 1 or electron 2 is partly within a localized MO close to one of the coupled nuclei and partly within another localized MO close to the other coupled nucleus (cases LLH and DVH, Figure 3, parts a and b). It does not matter whether both localized MOs are bonding or antibonding orbitals.

Considering *coupling pathways* containing only σ_1 or σ_2 and σ_1^* or σ_2^*, there is a fourth typical case where electron 1 is in both one occupied LMO and one virtual LMO close to only one nucleus but electron 2 is taken partially in a LMO that is close to one nucleus and partially in a LMO that is close to the other nucleus (case LVH, Figure 3d), which correspond to the following integral:

$$H_{\sigma_1\sigma_1*,\sigma_1\sigma_2*} = \int \sigma_1^*(1)\sigma_1(1)r_{12}^{-1}\sigma_2^*(2)\sigma_1(2)\, d\mathbf{r}_1\, d\mathbf{r}_2 \quad (37)$$

For *G* and *H* integrals where both electrons 1 and 2 are placed in MOs that belong to the same spatial region of the molecule they will not show a Karplus-type behavior (case DLH, Figure 3c).

Finally, there is another typical *coupling pathway* that follows a pattern similar to the case b): $\sigma_1\,\sigma_2^*\,\sigma_2\,\sigma_1^*$. In this case the two-electron integral *H* (*G*) has the same behavior as the integral *G* (*H*) in case b.

In Figure 6, the θ dependence of $V_{\sigma_1\sigma_1*,X(Y)}$ and $V_{\sigma_1\sigma_2*,X(Y)}$ are shown. Nonlocal "perturbators" have a Karplus-type behavior, but this is not the case for local perturbators.

At this point it is worthwhile to note that, as seen in Figures 5 and 6, the Karplus-type curves have a minimum very close to zero; on the other hand, the non-Karplus-type curves have a minimum rather farther from zero.

The analysis in this subsection could imply that the Karplus curve should arise only when we consider electronic correlation. This means that at RPA level of approach this will happen when including the two-electron integrals *G* and *H*. Then a natural question which follows from this analysis is: What would happen at the zeroth-order level of approach (ZOA)?

Hyperconjugation

J. Phys. Chem. A, Vol. 108, No. 29, 2004 **6237**
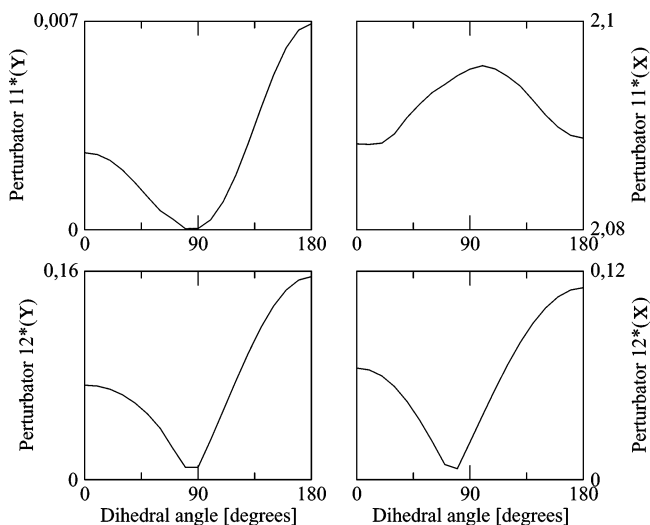
Figure 6. Perturbators $\sigma_1\sigma_1^*$ and $\sigma_1\sigma_2^*$ on nuclei X and Y respectively for cases a–c with X = Y = Sn.
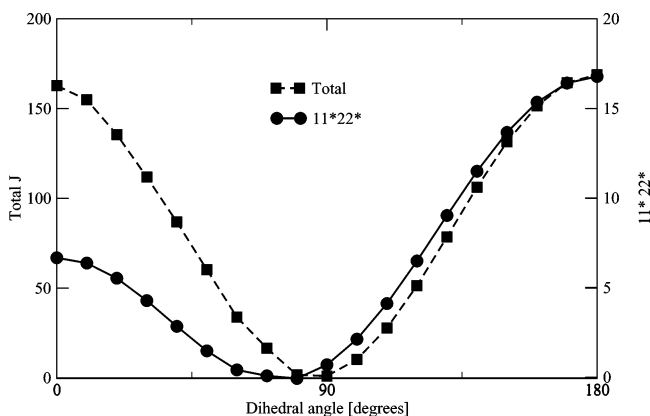
Figure 7. Total J and $\sigma_1\sigma_1^*,\sigma_2\sigma_2^*$ (11*22*) *coupling pathway* in Hertz at zeroth-order for X = Y = Sn.
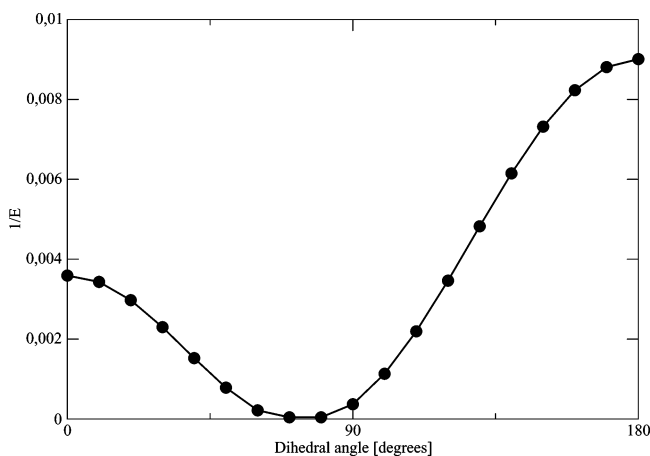
Figure 8. $(\epsilon_{\sigma_1}* - \epsilon_{\sigma_1})^{-1}$ corresponding to $\sigma_1\sigma_1^*,\sigma_2\sigma_2^*$ for X = Y = Sn.

3.4. Contributions at the Zeroth-Order Level. In ref 7 it was shown that the vicinal J coupling follows a Karplus curve when calculated within the finite-perturbation methodology. In this formulation, electronic correlation is included.

Within our scheme, the ZOA level of approach does not contain electronic correlation. Shall we expect a Karplus curve anyway? In Figures 7 and 8, we show the behavior for the total J coupling, the main coupling pathway ($\sigma_1\sigma_1^*$, $\sigma_2\sigma_2^*$) and the $\mathbf{E}^{-1}$ contribution at ZOA level of approach. It is nicely seen

that the total J is symmetric for θ between 0 and 180°. The main *coupling pathway* follows a Karplus curve but its origin is on the $\mathbf{E}^{-1}$ contribution and its magnitude is around 10% of the total value.

At the RPA level of approach the principal propagator in the basis of localized MOs can be written as

$$\mathbf{P} = \mathbf{E}_d^{-1}(\mathbf{I} + \mathbf{E}_{nd}\mathbf{E}_d^{-1} + ...)(\mathbf{I} + \mathbf{NE}^{-1} + ...) \quad (38)$$

where the matrix $\mathbf{I}$ is the diagonal unity matrix and $\mathbf{E}$ was divided in its diagonal and nondiagonal parts on the rhs of eq 38.

The principal propagator of eq 38 can then be reduced to

$$\mathbf{P}_{ia,jb}^{ZOA} = \sum_{rs}\{[\mathbf{E}_d^{-1}(\mathbf{I} + \mathbf{E}_{nd}\mathbf{E}_d^{-1} + ...)]_{ia,rs}\mathbf{I}_{rs,jb}\} \quad (39)$$

when considered at ZOA level. In this way

$$\mathbf{P}_{ia,jb}^{ZOA} \simeq (\mathbf{E}_d^{-1})_{ia,ia} \quad (40)$$

because for each matrix elements $\mathbf{E}_{nd} \ll \mathbf{E}_d$.

It is also observed that at ZOA level of approach the total J coupling is symmetric in θ and this result is due to the fact that "perturbators" corresponding to symmetric coupling pathways contribute with different sign.

4. Concluding Remarks

Response methods are powerful tools for searching the physics that underlies NMR J couplings. In this work the polarization propagator method through the (semiempirical) CLOPPA scheme was applied to a novel analysis of the dihedral-angle, θ, dependence of the vicinal NMR-J couplings, usually known as Karplus curve. Different pairs of coupled nuclei (X,Y = C, Si, Sn, Pb) belonging to the $XH_3-C_2H_4-YH_3$ molecular model were studied. The FC term is by far the largest one for these couplings. So this was the only one term analyzed.

We found out that each *coupling pathway* with independence of the particular selected coupled nuclei, follows the same pattern concerning their θ- dependence. So the functional θ dependence of J^{FC} for the above-mentioned model compounds is based on the same electronic mechanism.

A few years ago we developed a methodology that permit us to obtain the matrix elements of the principal propagator matrix as a power series where two kind of two-electron integrals, G and H are placed in the numerator. We analyzed the behavior of that two integrals G and H corresponding to different *coupling pathways* and found out that they also follow a Karplus curve when the electron one and/or the electron two are placed simultaneously in molecular regions which are close to both coupled nuclei. This means that there is an hyperconjugative electronic mechanism involved though of a different kind compared with previous studies; we call them *hyperconjugation of the second kind*, due to the fact that it involves two simultaneous electronic excitations. In the case of the main *coupling pathway* both integrals G and H follow a Karplus curve. We named this particular electronic mechanism as local local hyperconjugative, LLH, which means that electron one (two) is excited from the occupied LMO that belongs to the σ_1 (σ_2) bond to the unoccupied LMO σ_1^* (σ_2^*) and both are excited simultaneously. Analyzing the integrals G and H, it is observed that both electron one and electron two are included in such a way that each one of them belongs to two different molecular bonds that contain the nucleus X or Y.

From the analysis of some other integrals G and H belonging to typical *coupling pathways*, it follows that the θ Karplus-type dependence arises when one or both electrons are taken in LMOs belonging to two different molecular regions which involve the coupled nuclei. When both electrons are in LMOs that belongs to the same region, integral G or H has a θ dependence that is not of a Karplus-type.

Given that the matrix elements which belong to the principal propagator matrix are defined entirely by the unperturbed electronic molecular system, it follows that the main stream lines for transmitting (through electrons) the J couplings are given by the unperturbed electronic system.

Previous works on the electronic origin of dihedral angular dependence of vicinal J couplings have shown that hyperconjugation (of the *first kind*) plays an important but not the main role. Within the NJC theoretical model, the principal mechanism which produces the Karplus curve was related to a modification of the electronic spin density due to the external magnetic perturbation originated on the interaction of nuclear spins with their surrounding electron and transmitted by an steric orthogonalization of the NLMO. Given that this analysis was based on a completely different methodology, it is not possible to obtain any related analytic expressions for comparison. In any case, we can argue that the physics that underlies this nuclear spin coupling should be related to the propagation which the principal propagator takes into account. When the geometry of the molecule is allowed to be modified by varying the dihedral angle, the overlap between the LMOs which appear in the calculation of G and H will also vary. It seems that this overlapping is such that its contribution follows a Karplus curve. This is implied also in the mechanism proposed by Weinhold and co-workers.

After the finding that the two-electron integrals corresponding to the RPA level of approach within polarization propagator schemes are the factors which contain the information about the dependence of vicinal J with θ, we asked ourselves whether this is an effect arising from electronic correlation or not. This question was not considered in the application of previous schemes. Then we studied the variation of each *coupling pathway* at what we call the zeroth-order level of approach. This means a level where electronic correlation is not included in the calculation of the property. We observe that in this case the angular dependence comes from nonlocal "perturbators" and also from the inverse of the excitation energies. They contribute in such a way that the J value is symmetric even though each *coupling pathway* obeys a Karplus functional dependence with θ.

The mechanism named here as hyperconjugation of a *second kind* can be understood as related to the probability amplitude that two electrons be delocalized simultaneously from two occupied MOs to two virtual MOs; of special importance for NMR J are that excitations concerning two pairs of MOs that are localized in different regions of the molecule like the two simultaneous excitations $\sigma_1 \rightarrow \sigma_1^*$, $\sigma_2 \rightarrow \sigma_2^*$. These excitations arise from the hyperfine interaction at the site of each coupled nuclei when the FC mechanism is taken into account.

References and Notes

(1) Karplus, M. *J. Chem. Phys.* **1959**, *30* 11.
(2) Karplus, M. *J. Am. Chem. Soc.* **1963**, *85*, 2870.
(3) Contreras, R. H.; Peralta, J. E. *Prog. Nuc. Magn. Reson.* **2000**, *37*, 321.
(4) Mitchell, T. N.; Kowall, B. *Magn. Reson. Chem.* **1995**, *33*, 325.
(5) Case, C.; Scheurer, D. A.; Bruschweiler, R. *J. Am. Chem. Soc.* **2000**, *122*, 10390.
(6) Pophristic, V.; Goodman, L. *Nature* **2001**, *411*, 565.
(7) Wilkens, S. J.; Westler, J. L.; Markley, J. L.; Weinhold. F. *J. Am. Chem. Soc.* **2001**, *123*, 12026.
(8) Esteban, A. L.; Galache, M. P.; Mora, F.; Diez, E.; Casanueva, J.; San Fabian, J.; Barone, V.; Peralta, J. E.; Contreras, R. H. *J. Phys. Chem. A* **2001**, *105*, 5298.
(9) Aucar, G. A.; Contreras, R. H. *J. Magn. Reson.* **1991**, *93*, 413.
(10) Aucar, G. A.; Botek, E. L.; Gómez, S. B.; Sproviero, E.; Contreras, R. H. *J. Organomet. Chem.* **1996**, *524*, 1.
(11) Botek, E. L.; Aucar, G. A.; Cory, M.; Zerner, M. *J. Organomet. Chem.* **2000**, *598*, 193.
(12) Peruchena, N. M.; Sosa, G. L.; Aucar, G. A.; Contreras, R. H. *J. Mol. Struct. (THEOCHEM)* **1995**, *330*, 211.
(13) Diz, A. C.; Giribet, C. G.; Ruiz de Azúa, M. C.; Contreras, R. H. *Int. J. Quantum Chem.* **1990**, *37*, 663.
(14) Contreras, R. H.; Ruiz de Azúa, M. C.; Giribet, C. G.; Aucar, G. A.; Lobayan, R. M. *J. Mol. Struct. (THEOCHEM)* **1993**, *284*, 249.
(15) Oddershede, J.; Jørgensen, P.; Yeager, D. L. *Comput. Phys. Rep.* **1985**, *2*, 33.
(16) Gómez, C. A.; Provasi, P. F.; Aucar, G. A. *J. Mol. Struct. (THEOCHEM).* **2001**, *584*, 159.
(17) Zubarev, D. N. D. N. *Usp. Fiz. Nauk, (Engl. Transl.: Sov. Phys Usp., 3)* **1960**, *324−345*, 71.
(18) Oddershede, J. *Methods Comput. Mol. Phys.* **1997**, p 249.
(19) Lehman, H. *Nuovo Cimento* **1954**, *11*, 342.
(20) Aucar, G. A. *Chem. Phys. Lett.* **1995**, *254*, 13.
(21) Pyykko, P.; Wiesenfeld, L. *Mol. Phys.* **1981**, *43*, 557.
(22) Olsen, J.; Jensen, H. J. A.; Jorgensen, P. *J. Comput. Phys.* **1988**, *74*, 265.
(23) Reed, A. E.; Curtiss, L. A.; Weinhold, F. *Chem. Rev.* **1988**, *88*, 899.
(24) Barone, V.; Peralta, J. E.; Contreras, R. H.; Sosnin, A. V.; Krivdin, L. B. *Magn. Reson. Chem.* **2001**, *39*, 600.
(25) Peralta, J. E.; Contreras, R. H.; Snyder, J. P. *J. Chem. Soc., Chem. Commun.* **2000**, page 2025.
(26) Barfield, M.; Karplus, M. *J. Am. Chem. Soc.* **1969**, *91*, 1.
(27) Stewart. J. J. P. *J. Computer-aided Mol. Design* **1990**, *4*, 1.
(28) Dewar, M. J. S.; Thiel, W. *J. Am. Chem. Soc.* **1977**, *99*, 4899.